Terrestrial Organic Carbon inputs to the Oceans - II

Some additional light reading:

- Guo et al., 2004. Characterization of Siberian Arctic coastal sediments: Implications for terrestrial organic carbon export. Global Biogeochemical Cycles, 18, GB1036.
- Blair et al., 2004. From bedrock to burial: the evolution of particulate organic carbon across coupled watershed-continental margin systems. Mar. Chem. 92, 141-156.

Carbon isotopic compositions of leaf wax biomarkers

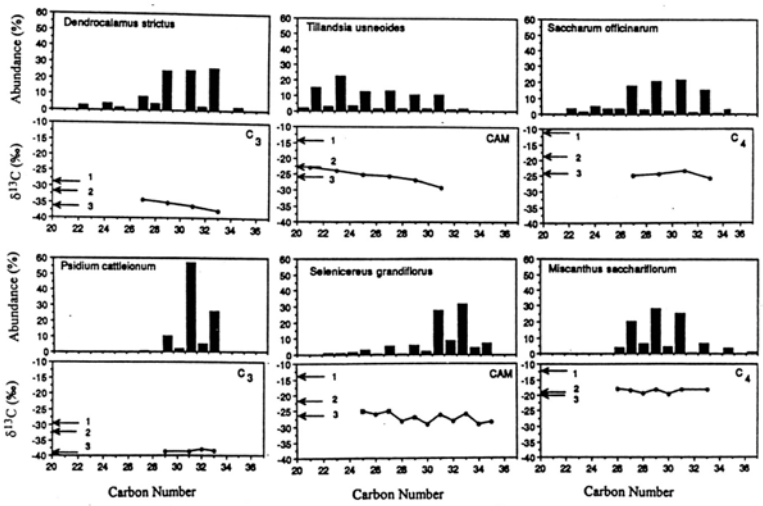

Fig. 1. Individual $\delta^{13}C$ values (‰ vs PDB) and relative abundances (% of total alkane fraction) vs *n*-alkane carbon number for plant waxes extracted from representative plants of different CO_2 metabolisms. 1, $\delta^{13}C$ value for leaf total tissue; 2, $\delta^{13}C$ value for total surface lipid extract; 3, weighted mean average $\delta^{13}C$ value for individual *n*-alkanes.

Long range transport and preservation of plant wax alkanes in marine sediments

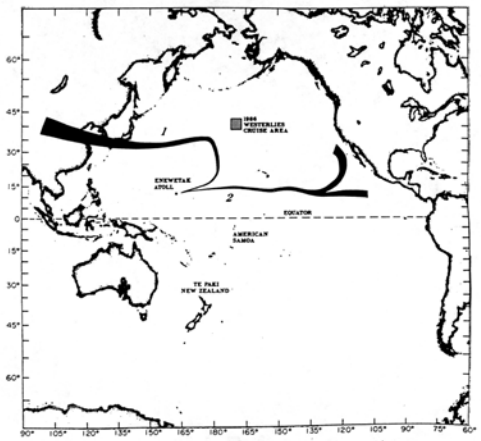

Fig. 1. Locations of the major SEAREX sampling sites and some of the typical air mass trajectories for the Enewetak site: (1) dry season; (2) wet season.

Gagosian and Peltzer

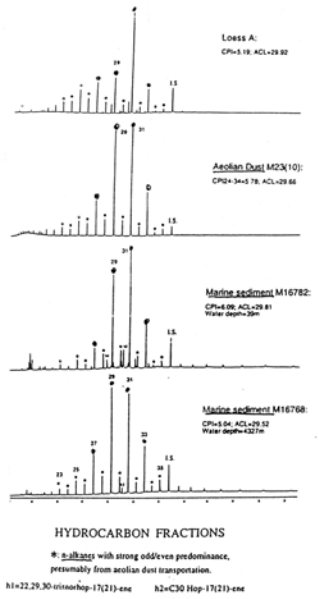

Eglinton (senior) et al

Influence of long-term degradation on isotopic composition of leaf-wax biomarker lipids

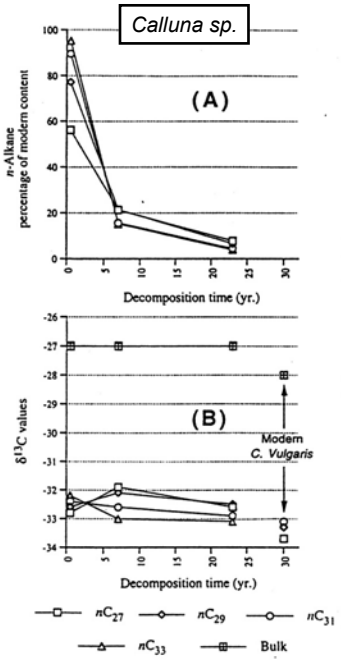

Vegetation zones of Africa (modern and past glacial)

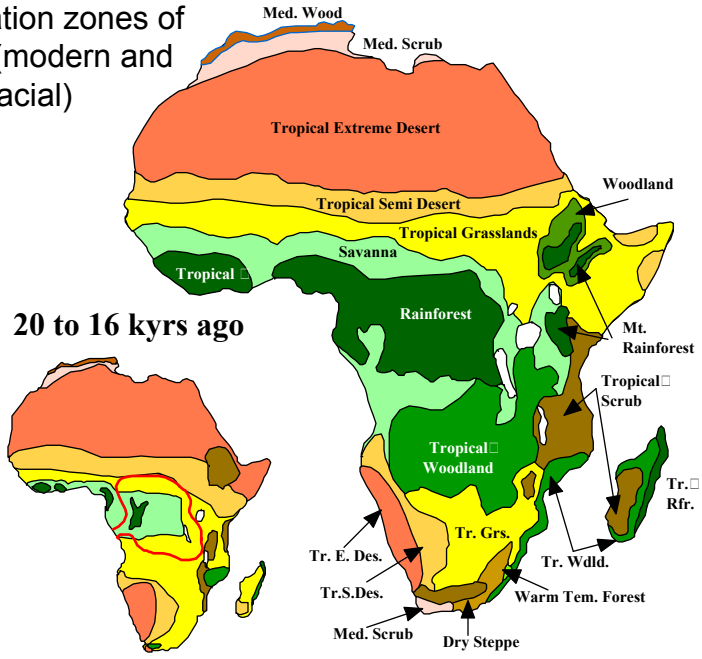

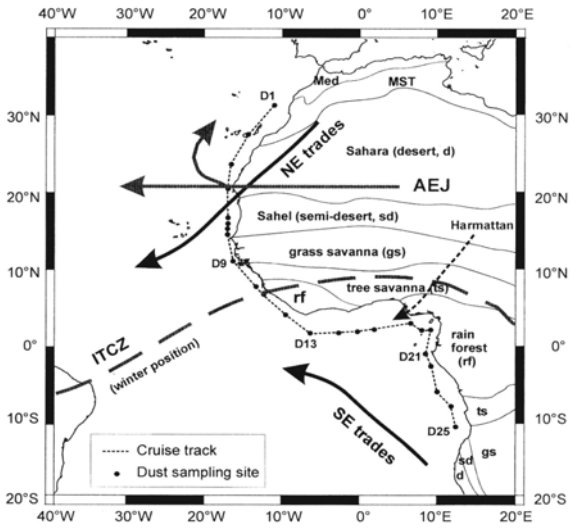

Fig. 1. Ship track and dust sampling sites of *RV Meteor* cruise M41/1 along the West African margin. Phytogeographical zonation of Africa is taken from White (1983): Med = Mediterranean vegetation; MST = Mediterranean–Saharan transition; d = desert; sd = semidesert; gs = grass savanna; ts = tree savanna; rf = rain forest. Major wind systems are drawn after Kalu (1979), Tetzlaff and Wolter (1980), and Sarnthein et al. (1981). Note that samples D19 and D20 were taken at almost the same location.

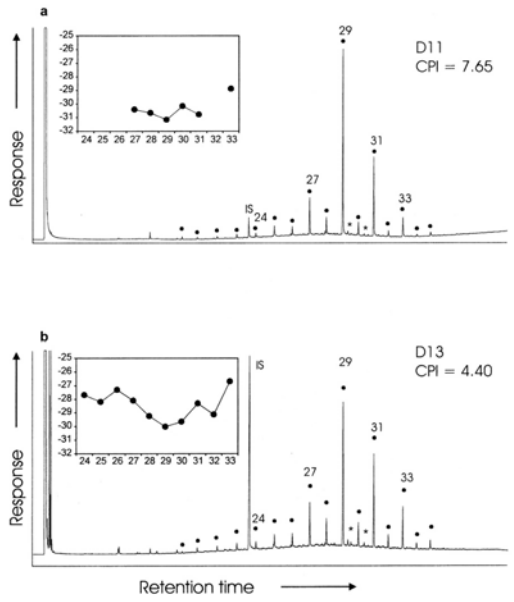

Fig. 3. Gas chromatographic traces of saturated hydrocarbon fractions of organic solvent extracts of aerosol samples with (a) a high and (b) a low CPI (above: D11, CPI = 7.65; below: D13, CPI = 4.40). Dots indicate *n*-alkanes, stars indicate 17α,21β(H)-hopanes. Insets show stable carbon isotopic compositions (in ‰) vs. chain-length of *n*-alkanes.

Distributions and $\delta^{13}C$ values of plant wax alkanes in aerosols

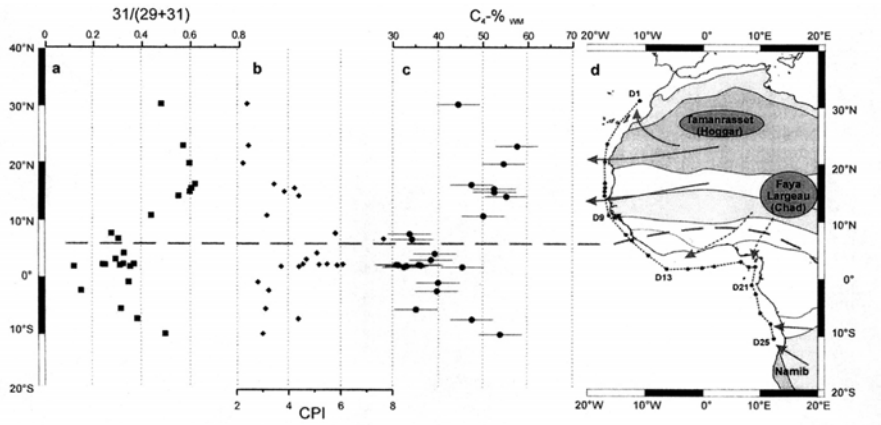

Fig. 4. (a) The variation in the ratio of the two dominant *n*-alkane homologues $n\text{-}C_{31}/(n\text{-}C_{29} + n\text{-}C_{31})$, (b) the CPI, and (c) the percentage of C_4 plant-derived *n*-alkanes in the aerosol samples vs. latitude. Ship track and sampling sites are shown. Note that sample D2 is missing. (d) Vegetation zones on the continent with mixed C_3/C_4 plant vegetation are light shaded, the Sahara and Namib desert with sparse but predominant C_4 plant vegetation are dark shaded. Major dust source regions and schematic transport pathways are indicated. The gray stippled line indicates the position of the ITCZ.

Plant wax (C_{29} *n*-alkane) carbon isotopes of African dust and E-Atlantic surface sediments

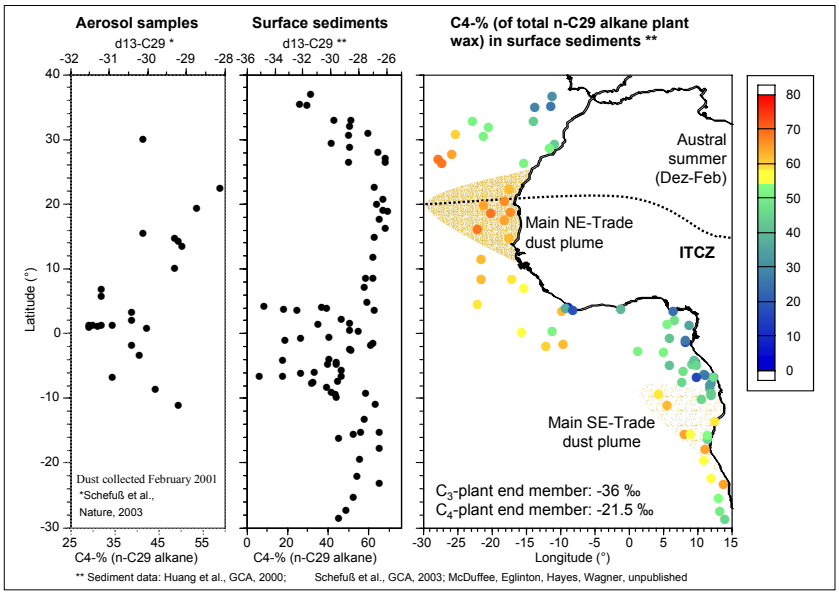

Carbon isotopic composition of dustfall sample off NW Africa

Fractions	Concn. (gdw basis)	$\delta^{13}C$ (‰)	$\Delta^{14}C$ (‰)	^{14}C age (yr BP)
Total Organic Carbon	1.02 %	-18.93	-149.6	1260 ± 40
Black Carbon	0.24 %	-15.13	-231.7	2070 ± 35
Plant wax alcohols	12 μg	-27.9	-80.8	649 ± 143

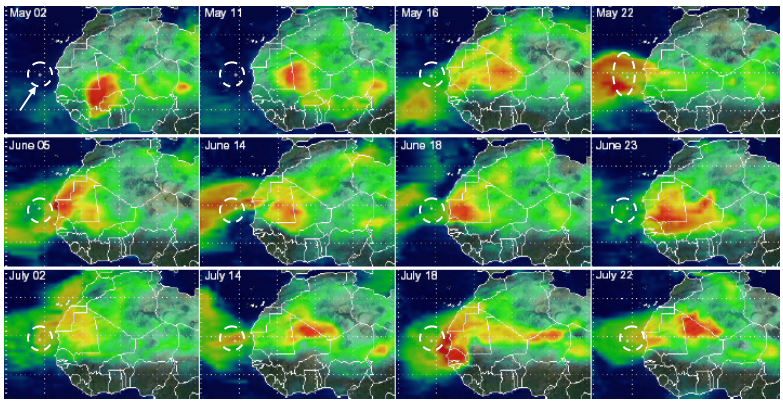

Eglinton et al., G³, 2002

Variations in terrestrial vegetation over geologic time

Isotopic compositions of Bengal fan sediments and the emergence of C4 plants

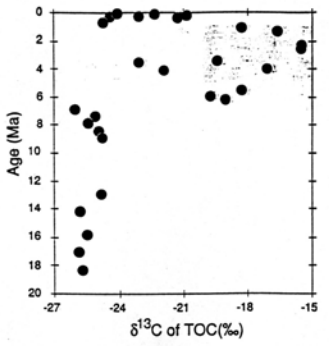

FIG. 2. $\delta^{13}C$ of TOC in Bengal Fan sediments plotted against age in Holes 717C and 718B. Data are available upon request to the authors or in NOAA data base. The increase of $\delta^{13}C$ values at *ca.* 7 Ma reflects the increase of the C4/C3 plant ratio in the source of the organic matter. The $\delta^{13}C$ increase near 7 Ma closely parallels that observed in paleosol studies in the Himalayan foreland (e.g., CERLING, et al., 1993), but the decrease after 0.9 Ma is not observed in the paleosol data. Variations in $\delta^{13}C$ are correlated with variations in sedimentation rate, grain size and clay mineralogy (Fig. 1).

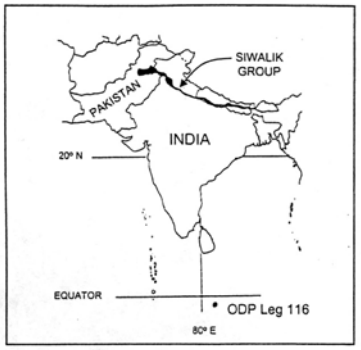

Fig. 1. Map of the Indian subcontinent showing outcrop pattern of Siwalik Group and sample localities for both paleosol and marine sediments (insert map).

Isotopic compositions of Bengal fan sediments and the emergence of C4 plants

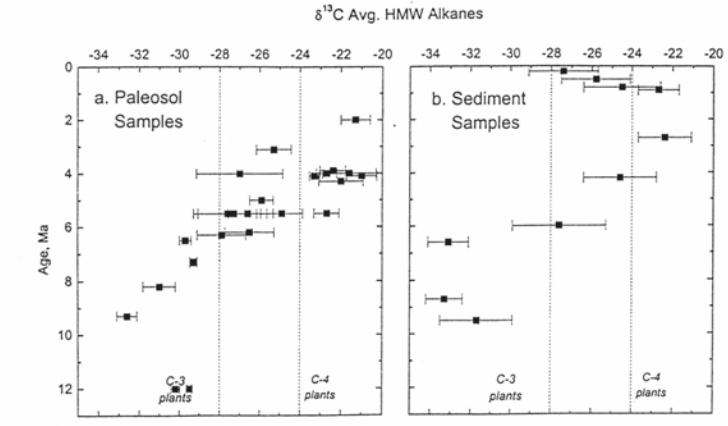

Fig. 6. $\delta^{13}C$ values representing the average of odd-carbon-numbered HMW alkanes plotted as a function of sample age for both the paleosol and sediment samples. Dotted line represent the approximate limits of *n*-alkane $\delta^{13}C$ values expected for C-3 and C-4 plants (see text and Table 14). Paleosol samples with evidence for significant contribution of *n*-alkanes from parent materials are not included.

Plant waxes, vegetation change, and human evolution

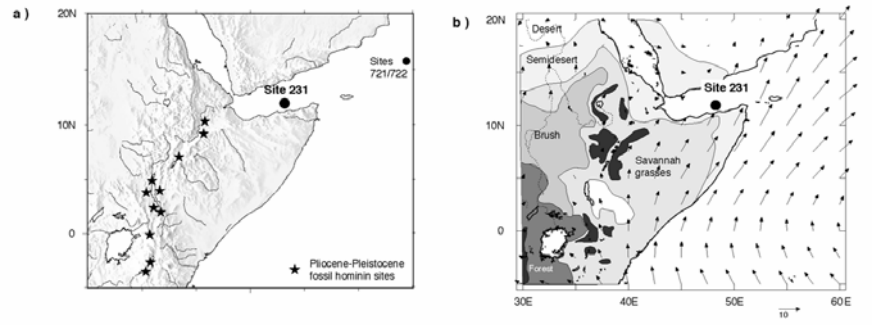

Ingram et al. in prep.

Plant waxes, vegetation change, and human evolution

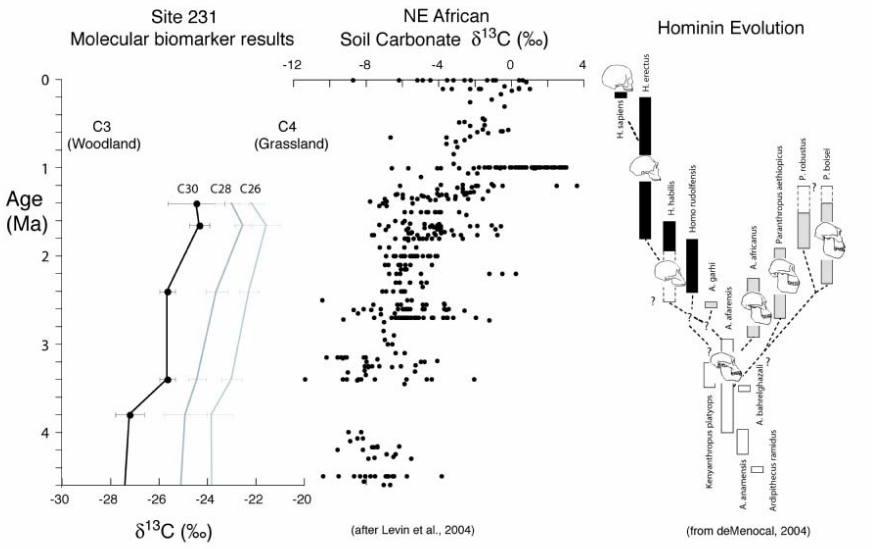

The origin of old OC in marine sediment core-tops (0-3 cm)

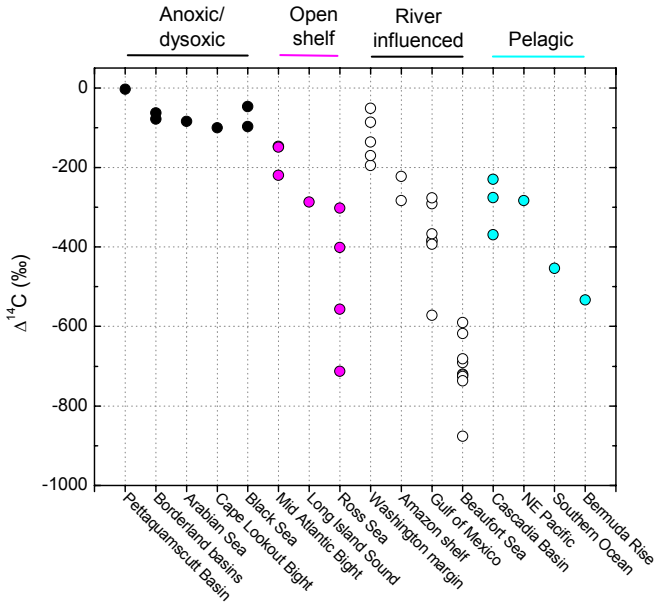

Radiocarbon content of SPOM from the Amazon River

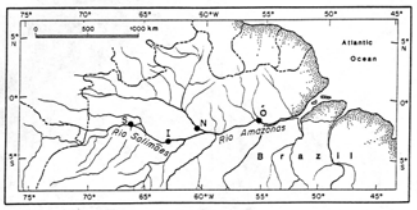

Fig. 1. Study area. CAMREX sampling sections are indicated by solid dots. Section identification abbreviations: S, Santo Antônio do Içá; I, Itapeúa; N, Rio Negro; O, Óbidos.

Table 1. $\Delta^{14}C$ values and minimum estimates of bomb carbon in individual samples of suspended particulate organic material (SPOM) and dissolved humic substances from the Amazon River. See (12) for analytical procedures. The $\Delta^{14}C$ of CO_2 in the atmosphere in 1983 was +234 ± 3 per mil (14).

Sample	$\Delta^{14}C$ (per mil)	Modern carbon* (%)	Minimum bomb carbon† (%)
Santo Antônio do Içá			
Coarse SPOM	+227 ± 14	123	32
Fine SPOM	+19 ± 19	102	5
Itapeúa			
Total humics	+283 ± 13	128	39
Rio Negro			
Humic acid	+141 ± 18	114	21
Fulvic acid	+344 ± 20	134	47
Total humics‡	+264 ± 15	126	37
Óbidos			
Humic acid	+180 ± 12	118	26
Fulvic acid	+290 ± 14	129	40
Total humics‡	+265 ± 12	127	37

*Percentage of the ^{14}C concentration of modern (1950) atmospheric CO_2. †A maximum value calculated from $[+750(\alpha/100) + (-20)(1 - \alpha/100)] = \Delta^{14}C_{max}$, where α is the percentage of bomb carbon. +750 represents the maximum $\Delta^{14}C$ for CO_2 in the equatorial atmosphere after atmospheric testing of nuclear weapons [estimated from (13)], and −20 corresponds to the $\Delta^{14}C$ of atmospheric CO_2 just before testing (20). ‡Calculated from the weight percent of organic carbon and the $\Delta^{14}C$ of the components humic and fulvic acids. Ratios of fulvic acid carbon to humic acid carbon for the Rio Negro and Óbidos samples are 1.55 and 3.42, respectively (11).

Hedges et al., 1986?

^{14}C variability in riverine suspended particulate organic matter

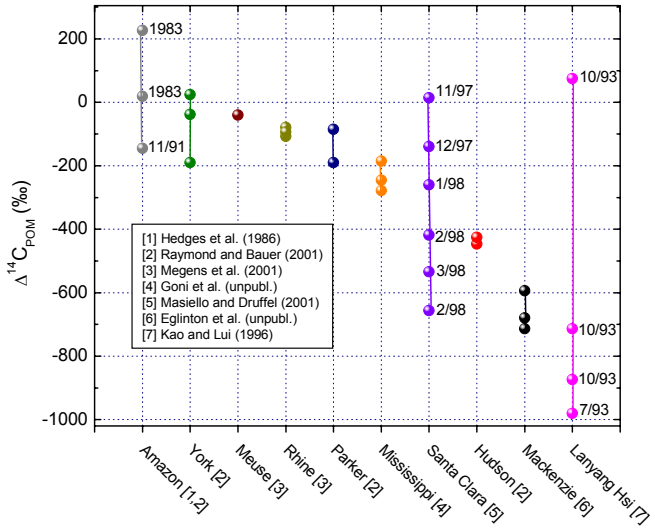

Factors controlling timescales of delivery of terrestrial organic carbon to the coastal ocean.

Mode of Delivery
- Riverine
- Aeolian
- Groundwater (DOC)

Characteristics of watershed
- Areal extent
- Topography
- Precipitation/Temperature
- Regional lithology
- Vegetation cover/type
- Anthropogenic activity (e.g., dams, levees).

^{14}C age variability in vascular plant biomarkers from Washington Margin surface (0-2 cm) sediments

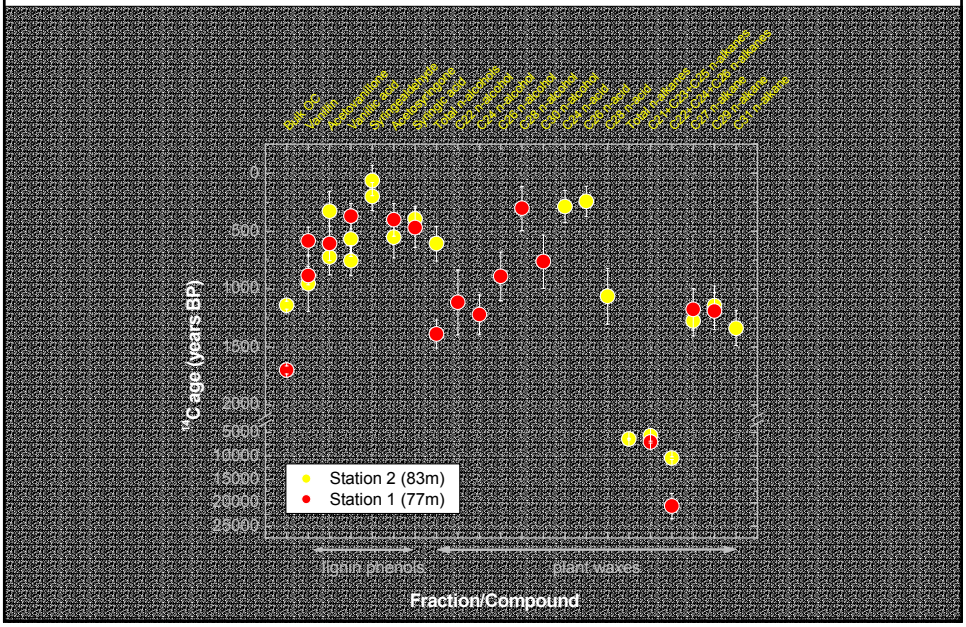

Importance of tropical mountainous river systems in terrigenous OC export to the oceans

Annual discharge (10^{12}gC yr^{-1}) of total OC of major world rivers to the oceans

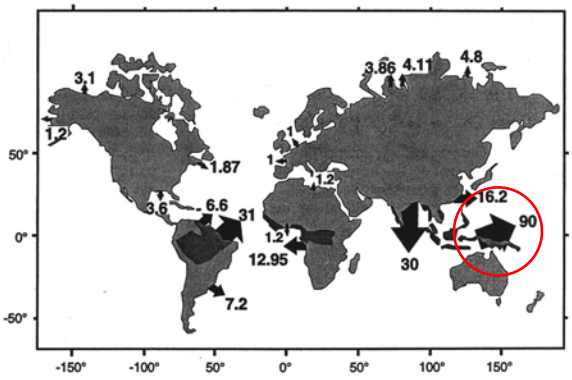

Small rivers on active margins supply > 40% of the fluvial sediments to the world's ocean

Milliman et al

Importance of tropical mountainous river systems in terrigenous OC export to the oceans

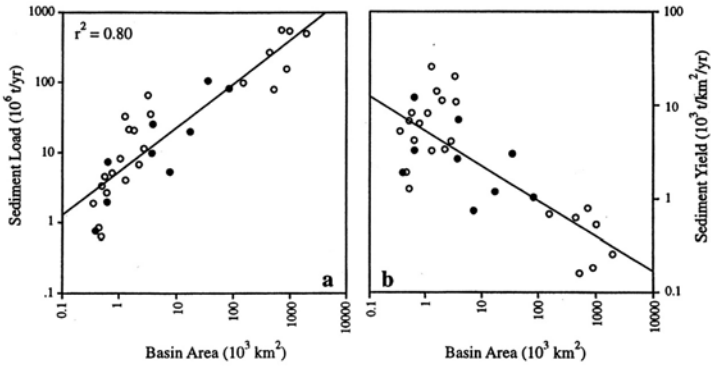

Fig. 1. Relationship between annual sediment load (a) and sediment yield (b) and basin area for various southeast Asian and Indonesian/Papua New Guinean humid (>500 mm y^{-1} run-off), mountain (>1000 m headwater elevation) rivers. Note that the East Indies rivers (Fly, Purari, Solo, Citamandy, Cimanuk, Cimuntur, Cilutung, Cijolang, and Agno; solid dots) have loads and yields very near values predicted based solely on southeast Asian river (open circles) algorithms; see text for further discussion. Data from Milliman and Syvitski (1992), somewhat modified by Milliman and Farnsworth (in prep.).

Terrigenous OC delivery and deposition on the Eel Margin

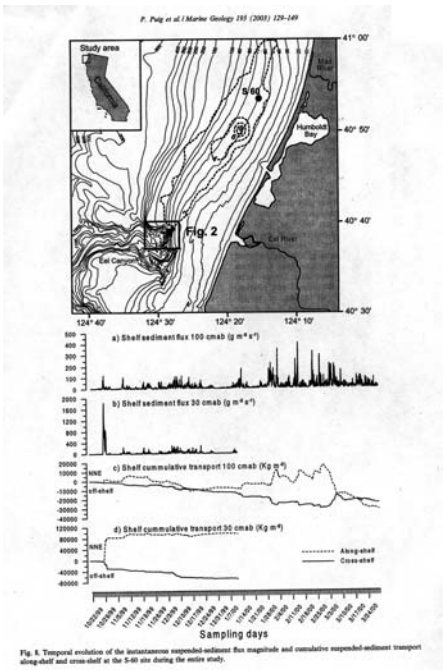

Terrigenous OC delivery and deposition on the Eel Margin

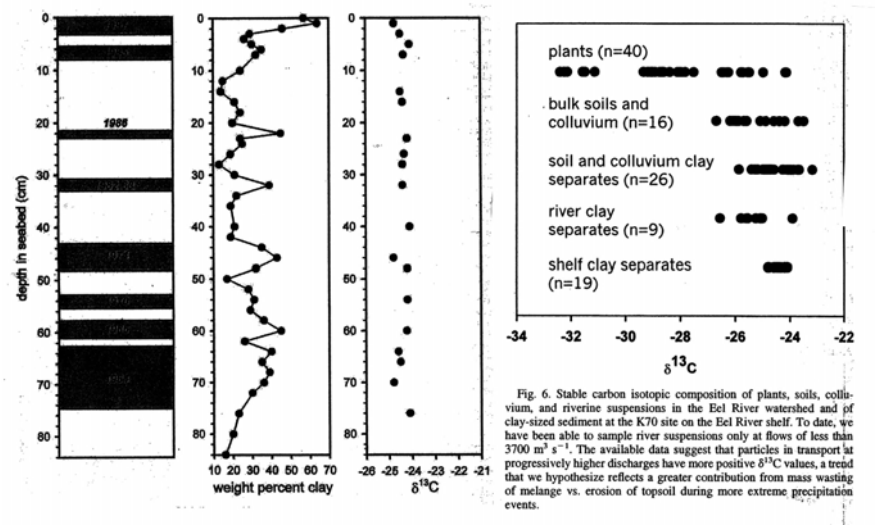

Fig. 6. Stable carbon isotopic composition of plants, soils, colluvium, and riverine suspensions in the Eel River watershed and of clay-sized sediment at the K70 site on the Eel River shelf. To date, we have been able to sample river suspensions only at flows of less than 3700 $m^3 s^{-1}$. The available data suggest that particles in transport at progressively higher discharges have more positive $\delta^{13}C$ values, a trend that we hypothesize reflects a greater contribution from mass wasting of melange vs. erosion of topsoil during more extreme precipitation events.

Compositional variations between organic matter sources and sinks in the Eel River-Margin system

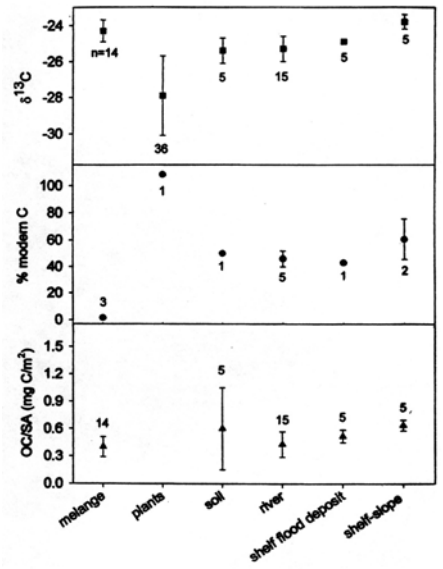

From Blair and Leithold

Influence of episodic delivery on the fate of terrestrial OC on the Eel shelf

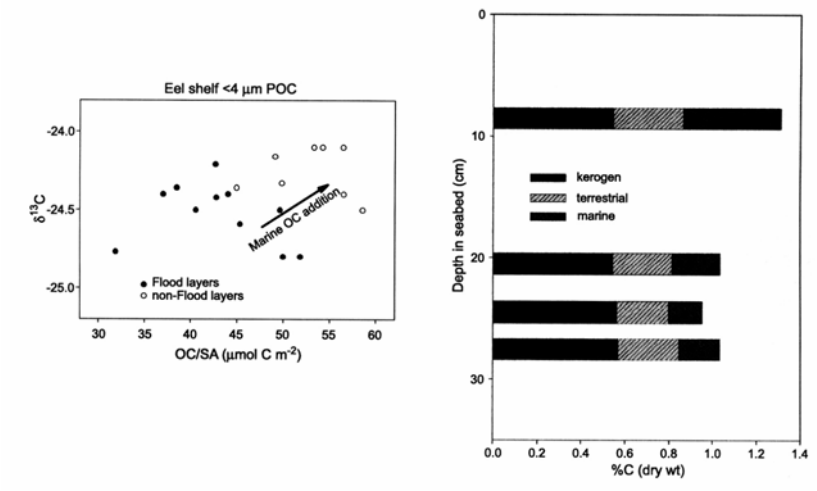

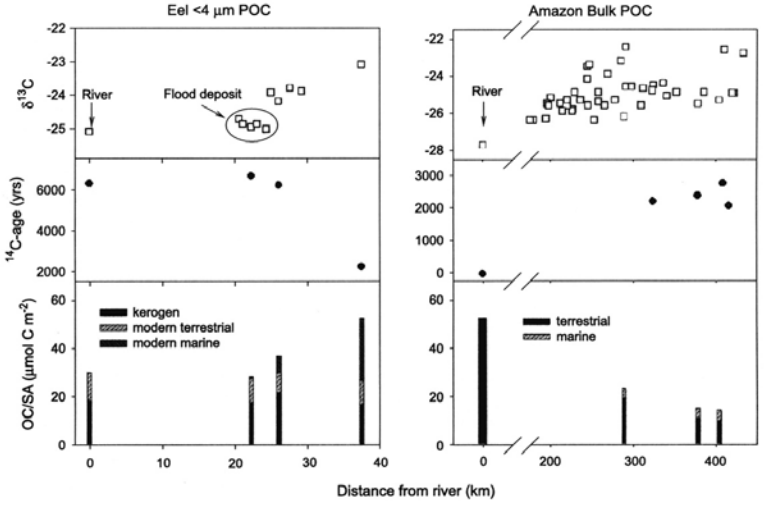

Conceptual model describing controls of watershed-continental margin processes on particulate OC export from river systems

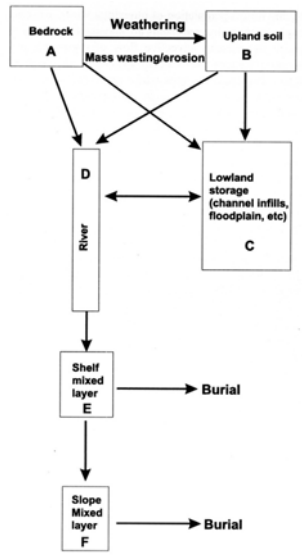

Fig. 1. Coupled watershed–seabed model describing the evolution of POC. Changes in POC content occur primarily in boxes; however, transport between reservoirs can result in hydrodynamic sorting and desorption of OC.

From Blair et al., 2004

Arctic Ocean

- Largest shelf area of all major oceans
- Numerous major rivers drain into Arctic Ocean
- Large terrestrial reservoirs of slowly cycling carbon (permafrost soils, sedimentary rocks)
- Dramatic seasonal variations in river discharge (spring freshet)
- Mechanisms of sediment dispersal from rivers (spill-over, ice rafting/keeling) that are distinct from low latitude river systems.
- Less active OC remineralization due to lower temps?

Terrestrial OC export from the Siberian Arctic

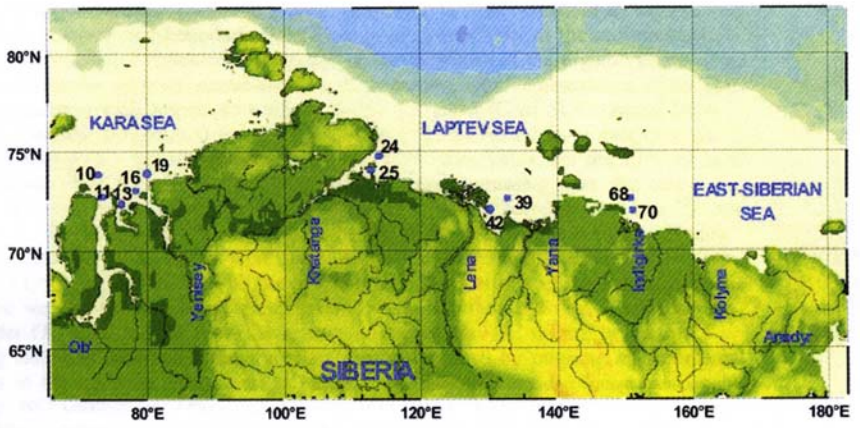

Map of the Siberian Arctic region and sampling locations.

Guo et al. 2004

Distribution of Permafrost in the Siberian Arctic

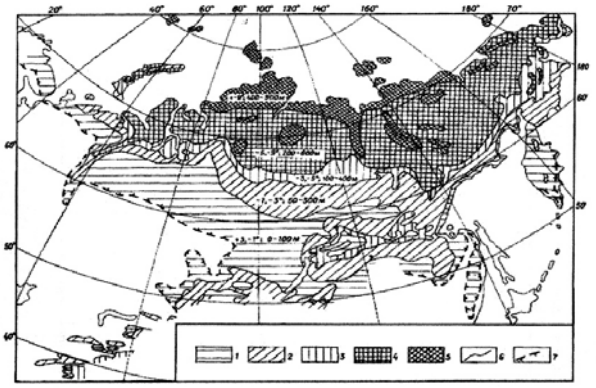

Figure 2. Distribution of permafrost zone increasing from west to east coast. Numbers given in key: 1: the zone of island permafrost with the mean temperature (T) from +3°C to −1°C, and thickness (H) from 0 to 100 m; 2–5: the zone of continuous permafrost with the different mean temperature and thickness: 2: T = from −1°C to −3°C, H = 50–300 m; 3: T = from −3°C to −5°C; 4: T = from −5°C to −9°C; 5: T < −9°C; 6: boundary between the different permafrost zones; and 7: the southern boundary of island permafrost distribution (boundary of the permafrost and permafrost islands regions are adopted from *Danilov* [1990]).

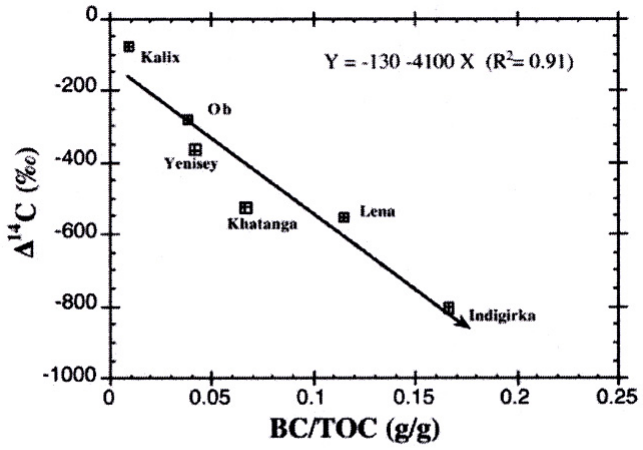

Relationship between $\Delta^{14}C$ values of sedimentary organic matter and the ratio of black carbon (BC) to total organic carbon (TOC) in the Siberian Arctic coast and the Kalix River. Note that the decreasing trend of $\Delta^{14}C$ with increasing BC/TOC ratio is from the west to the east coast.

The Mackenzie/Beaufort System

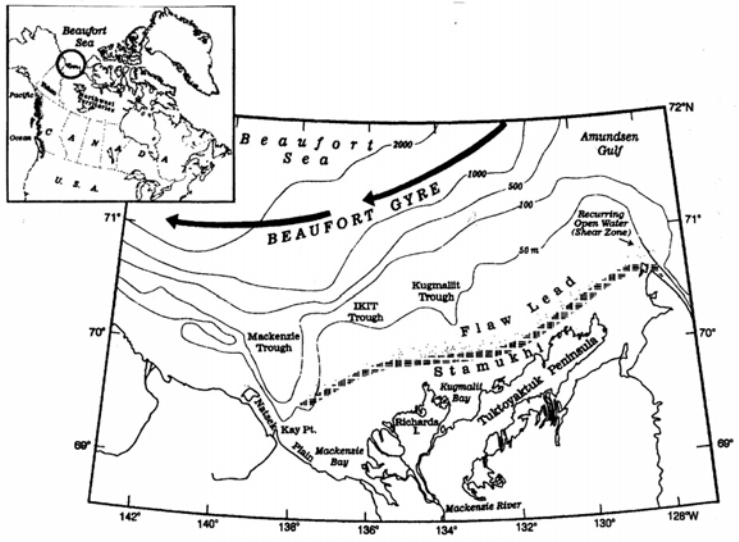

Fig. 1. Location map of the Mackenzie Shelf in the Canadian Beaufort Sea showing the various features discussed in the text.

Riverine delivery and transport of OC (Mackenzie/Beaufort)

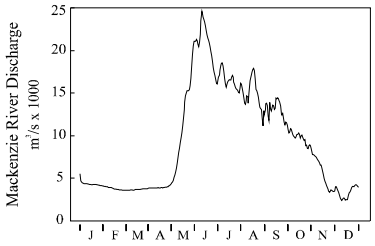

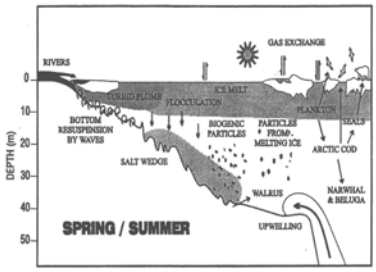

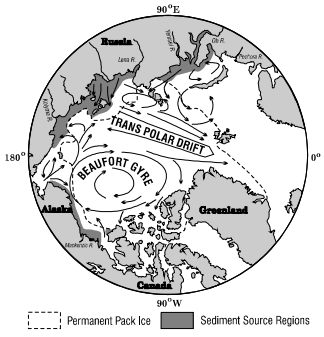

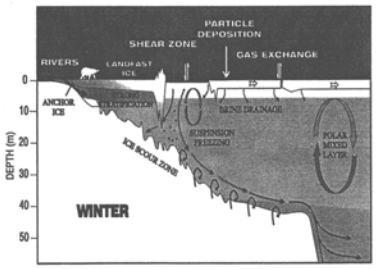

The Mackenzie Delta & Beaufort Sea

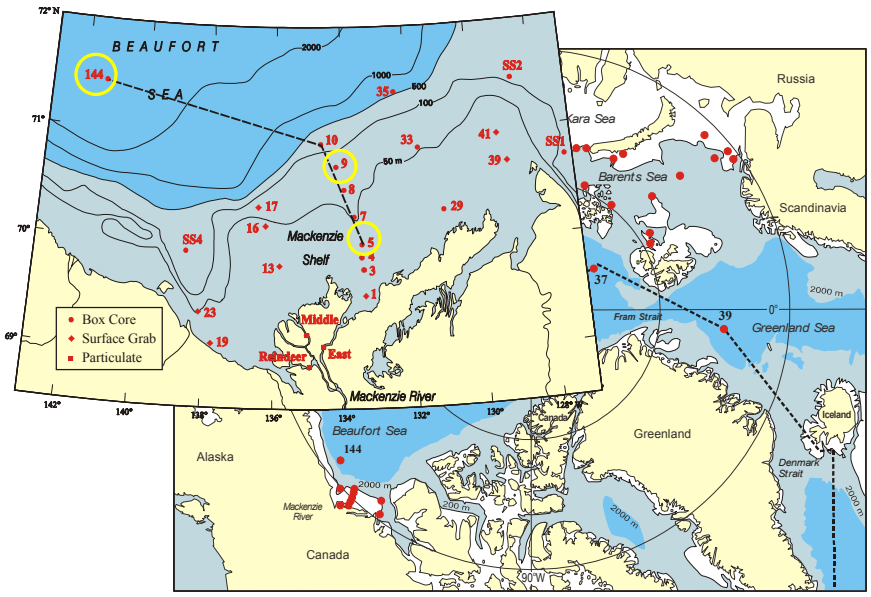

$\delta^{13}C$ compositions and ^{14}C ages of bulk OC in Mackenzie Delta/Beaufort Sea Core-top sediments

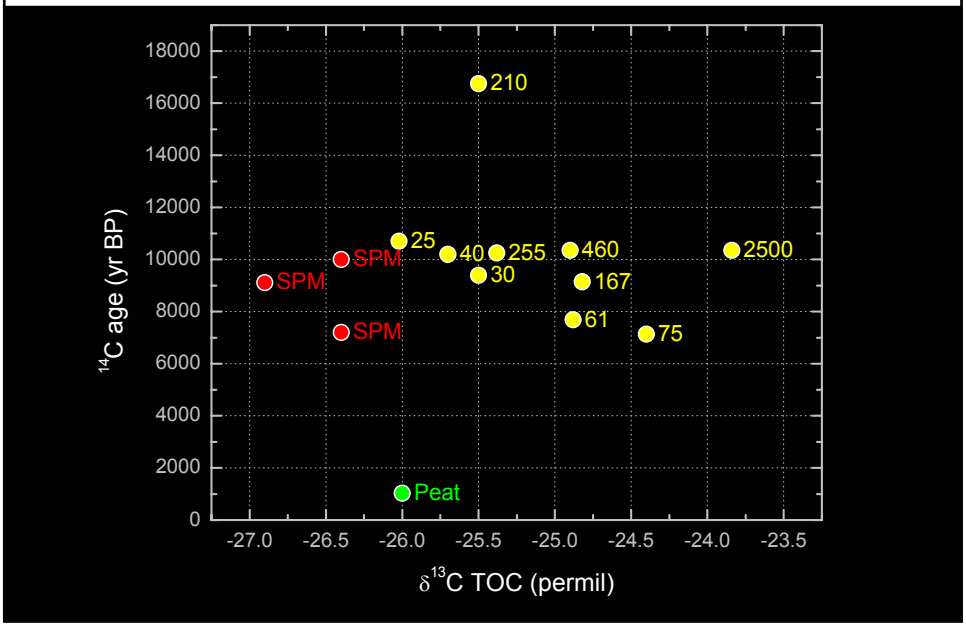

Geochemical Characteristics of OC in the Mackenzie/Beaufort system

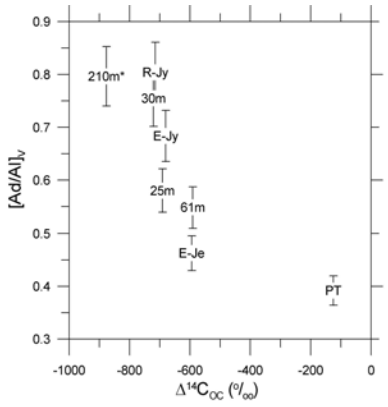

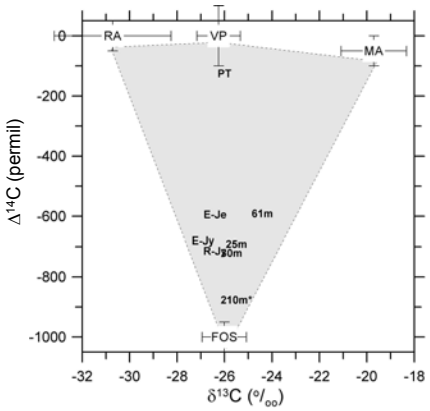

Goni et al. 2005

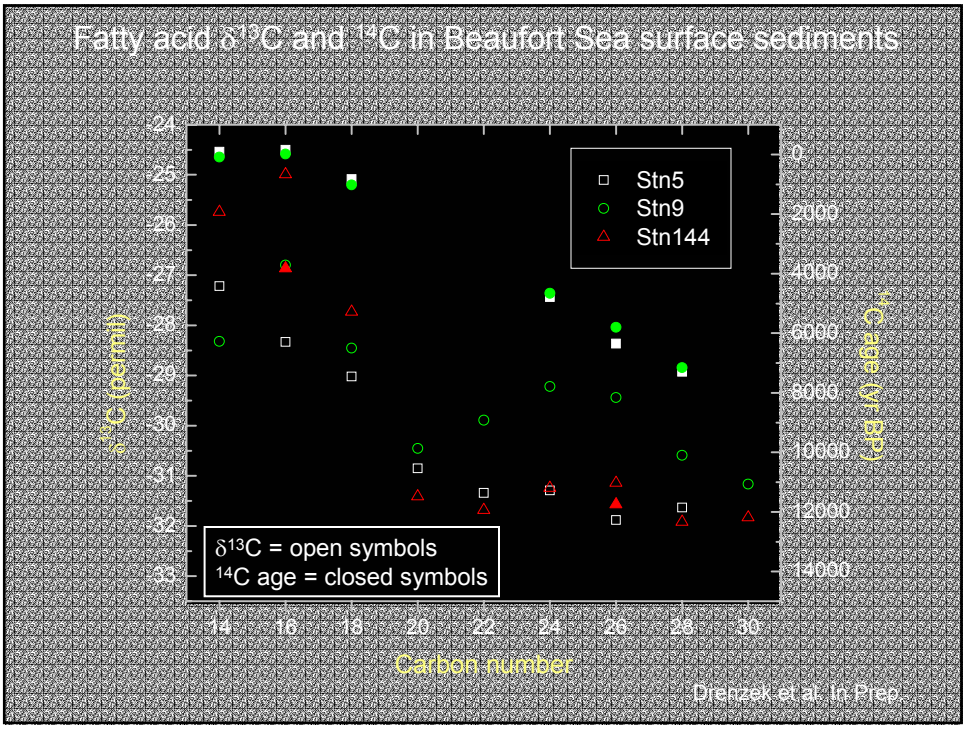
Fatty acid δ13C and 14C in Beaufort Sea surface sediments
δ13C (permil)
14C age (yr BP)
Stn5
Stn9
Stn144
δ13C = open symbols
14C age = closed symbols
Carbon number
Drenzek et al. In Prep

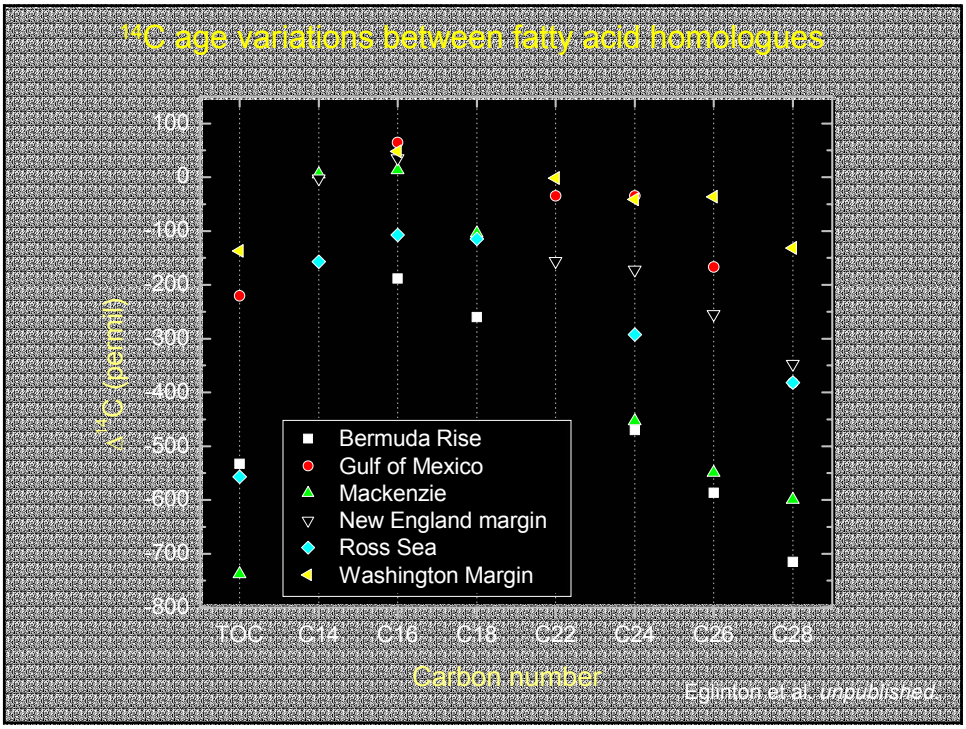
14C age variations between fatty acid homologues
Δ14C (permil)
Bermuda Rise
Gulf of Mexico
Mackenzie
New England margin
Ross Sea
Washington Margin
TOC
C14
C16
C18
C22
C24
C26
C28
Carbon number
Eglinton et al. unpublished

Some take-home points

- POC flux from rivers is sufficient to account for OC burial flux in marine sediments.
- Deltas sequester nearly half of the OC buried in the marine environment.
- Gross compositional characteristics ($\delta^{13}C$, C/N, OC:SA) of OC accumulating near the mouths of major river systems suggests efficient remineralization of terrestrial OC (esp. within estuaries, deltas).
- However, bulk parameters prone to uncertainty.
- Current estimates of riverine contributions to OC buried in marine sediments may be low due to:
  - Complicating influence of C4 (^{13}C-enriched) and soil-derived (low C/N) OC.
  - Underestimation of the importance of numerous, small mountainous rivers on active margins as sources of [old] terrigenous OC.
  - Lack of information on OC sources and burial in Arctic ocean sediments.
- Molecular markers can be used to better define input signatures, residence times (ages) of terrestrial OC, however quantification of this elusive pool of OC in marine sediments remains challenging.